2003

Temperature dependent kinetics of biotin carboxylase

Brett K. Lord
Louisiana State University and Agricultural and Mechanical College, blord1@lsu.edu

TEMPERATURE DEPENDENT KINETICS OF BIOTIN CARBOXYLASE

A Thesis
Submitted to the Graduate Faculty of the
Louisiana State University and
Agricultural and Mechanical College
in partial fulfillment of the
requirements for the degree of
Master of Science

in

The Department of Biological Sciences

by
Brett K. Lord
B.S., University of South Dakota, 1995
May 2003

ACKNOWLEDGEMENTS

If it weren't for the commitment and dedication of many people, none of this would have been possible. I would like to extend my gratitude to Dr. Grover Waldrop for the direction and guidance he has provided throughout this extremely short period of time of my graduate career. His commitment to my personal and professional development has never faltered, and his constant drive to "get data" allowed me to surpass my own expectations. I have been fortunate to have the opportunity to work in his lab.

I would also like to express my gratitude to Dr. Anne Grove and her lab for the valuable insights into the many aspects of my graduate work. Their assistance, knowledge and patience were one of the cornerstones that allowed me to conquer numerous problems and advance my research. I would also like to thank Dr. Sue Bartlett for supporting me in this pursuit to better myself personally and professionally.

To Keith Levert, Valerie Sloane, Tee Bordelon, and Mike Oldham, your daily discussions and invaluable insights into the general knowledge of conducting research and numerous breaks for humor is greatly appreciated and will always be remembered.

Most importantly, if it were not for the love and support of my family, none of this would have been possible. To my wife, Natalie, and my son, Braddock, I owe the greatest appreciation. Without your love and support, I would have never had the motivation to get where I am today. To my parents and to my wife's family, your support has been instrumental in the success of our whole family.

TABLE OF CONTENTS

LIST OF TABLES

LIST OF FIGURES

ABSTRACT

Acetyl-CoA carboxylase catalyzes the first committed step in long chain fatty acid biosynthesis. In *Escherichia coli*, the enzyme is composed of three distinct protein components: biotin carboxylase, biotin carboxyl carrier protein, and carboxytransferase. The biotin carboxylase component has served for many years as a model for mechanistic studies devoted toward understanding biotin-dependent carboxylases. Studies of the temperature dependence, temperature dependence of the kinetic solvent isotope effect and thermodynamics of biotin carboxylase are reported. Analysis of the van't Hoff plot in H_2O was biphasic showing an apparent transition temperature of 20°C, with corresponding $\Delta H°$ values of –4.55 ± 1.84 kcal/mol below the transition temperature and –1.59 ± 0.16 kcal/mol above the transition temperature, respectively, suggesting a conformational change is occurring at this temperature. Biphasic Arrhenius and Eyring plots in D_2O showed an apparent transition temperature at 25°C with corresponding E_a and $\Delta H^{\ddagger}$ values of 16.35 ± 0.90 kcal/mol and 15.86 ± 0.85 kcal/mol below the transition temperature, respectively, and E_a and $\Delta H^{\ddagger}$ values of 4.01 ± 1.15 kcal/mol and 3.37 ± 1.06 kcal/mol above the transition temperature, respectively. This break in the plots is suggestive of either a conformational change or a change in the rate-determining step occurring at 25°C. Kinetic solvent isotope effects were used to distinguish between these two possibilities. The results of the kinetic solvent isotope effect suggest a change in the rate-determining step as a function of temperature is occurring and is not due to a conformational change. Analysis of Arrhenius preexponential factors (A_H/A_D)

determined from the temperature dependence of the kinetic solvent isotope suggests both hydrogen and deuterium tunneling in biotin carboxylase.

CHAPTER 1

INTRODUCTION

1.1 Acetyl CoA Carboxylase. Acetyl CoA carboxylase catalyzes the first committed step in long chain fatty acid synthesis (Wakil *et al*., 1983), with the end product, malonyl CoA, being formed from acetyl CoA, ATP and bicarbonate. Found in all animals, plants and bacteria, acetyl CoA carboxylase is a biotin-dependent enzyme and the reaction occurs with the following two-step reaction mechanism (Lane *et al*., 1974).

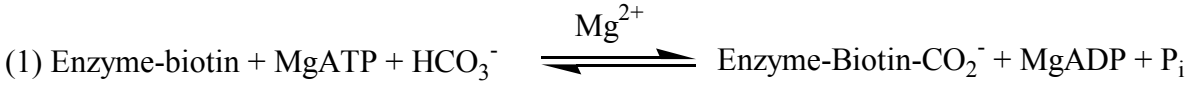

Acetyl CoA carboxylase from *E. coli* is composed of three distinct subunits which allows it to carry out these different reactions. Reaction 1, which is catalyzed by the biotin carboxylase subunit, involves the ATP-dependent carboxylation of biotin to form carboxybiotin through a carboxyphosphate intermediate. This is followed by the transfer of the carboxyl group to the 1′ nitrogen of biotin (Knowles, 1989). *In vivo*, biotin is attached to the biotin carboxyl carrier protein (designated as enzyme-biotin in reactions 1 and 2) through an amide bond to a specific lysine residue. In reaction 2 catalyzed by carboxyltransferase, the carboxyl group of carboxybiotin is transferred to acetyl CoA to form malonyl CoA. Animals contain all three subunits on a single polypeptide chain. Each protein of bacterial acetyl CoA carboxylase can be isolated and has been found to

retain activity. Moreover, both biotin carboxylase and carboxyltransferase utilize free biotin as a substrate, thus simplifying kinetic analysis of these two enzymes (Guchhait *et al*., 1974). Therefore, acetyl CoA carboxylase from *E. coli* has served as the model system for the studies of biotin-dependent carboxylases.

1.2 Biotin Carboxylase. Biotin carboxylase, encoded by the accC gene, remains the model system for studying biotin-dependent carboxylation reactions for several reasons. First, the gene encoding the enzyme has been cloned, sequenced and overexpressed, allowing for ample amounts of protein for physicochemical studies. The gene consists of a 1350-bp ORF which codes for a protein of ~50 kDa with 449 amino acids (Li & Cronan, 1992). Second, the crystal structure has been determined and remains the only three-dimensional model of a biotin-dependent carboxylase (Waldrop *et al*., 1994). The crystal structure confirmed that the enzyme is a homodimer. The homodimer of biotin carboxylase has two distinct active sites that do not contain residues from each monomer (known as a shared active site) as seen with other multisubunit enzymes such as aspartate transcarbamoylase (Wente & Schachman, 1987) and ribulose-1,5-bisphosphate carboxylase (Lorimer *et al*., 1987). However, work by Janiyani *et al.* (2001) using hybrid dimers of biotin carboxylase concluded that the two monomers do not function independently of one another.

The crystal structure of biotin carboxylase was determined to 2.4 Å resolution and showed that biotin carboxylase is arranged in three domains: an N-terminal domain, a B-domain and a C-terminal domain. The C-terminal domain was found to contain the active site and the B-domain was postulated to either interact with biotin carboxyl carrier

protein (BCCP), or act as a "cap" that clamps down on the active site when all of the substrates are positioned for catalysis (Waldrop *et al.,* 1994). Further work on the crystal structure of biotin carboxylase with ATP bound showed that a significant conformational change occurred in the B-domain of biotin carboxylase when ATP was bound, with an overall rotation ~ 45° and the movement of some atoms up to 8 Å (Thoden *et al.*, 2000). With this information, biotin carboxylase has been classified as a member of the ATP-grasp superfamily of proteins. The enzymes of this family share a structural homology which is consistent with each enzyme catalyzing an ATP-dependent ligation of a carboxyl group to an N or S atom via an acyl phosphate intermediate. Other enzymes in this family include D-ala:D-ala ligase, glutathione synthetase, succinyl CoA synthetase and carbamoyl-phosphate synthetase, to name a few (Galperin & Koonin, 1997).

1.3 Kinetic Studies of Biotin Carboxylase. In the absence of biotin, biotin carboxylase catalyzes the hydrolysis of ATP to ADP and Pi, in a bicarbonate-dependent manner, albeit at a very slow rate. However, upon the addition of biotin, the rate of ATP hydrolysis increases about 1100-fold (Lane *et al*., 1974). This significant increase in the reaction rate of one substrate caused by the binding of another substrate is called substrate-induced synergism (Bridger *et al*., 1968). One possible explanation for this relationship is that in the absence of biotin, ATP binds to the enzyme in a large number of non-productive binding orientations, and with the binding of biotin to the enzyme, these non-productive binding orientations are reduced, thus increasing the catalytic rate.

Combining the kinetic observations of Blanchard *et al.* (1999) with structural studies, a mechanism can be proposed in which ATP binds to the enzyme, causing a major

conformational change, followed by bicarbonate, and then the binding of biotin, causing an increase in the rate of ATP hydrolysis with little change in the conformation of the enzyme (Waldrop *et al*., 1994). The question was then asked: how is biotin able to stimulate the rate of ATP hydrolysis if not through conformational changes? Work on site-directed mutagenesis of the active site of biotin carboxylase by Sloane *et al.* (2001) suggested that the binding of biotin to the enzyme positions the substrates into a more reactive conformation. The lack of a large conformational change in biotin carboxylase upon binding biotin is consistent with its high K_m for biotin (134 mM). The binding energy was calculated to have a value of 1.2 kcal/mol, which is not suggestive of a large conformational change. Sloane *et al.* suggested that biotin only promotes small conformational changes in the enzyme by aligning the substrates for catalysis. Recent studies on hydrogen tunneling in dehydrogenases have found a correlation between protein dynamics and enzymatic activity. Hydrogen tunneling is the phenomenon by which a particle can pass through an activation barrier as opposed to over it. One example is the work conducted on isocitrate dehydrogenase, to which the binding of its substrate, isocitrate, induces shifts of less than an angstrom in the amino acid side chains of the active site. This seemingly insignificant change in conformation is related to a rate increase of many orders of magnitude (Koshland 1994 & 1998). Thus, it is plausible that the subtle dynamic behavior of biotin carboxylase is enough to generate the large increase in rate of ATP hydrolysis upon the binding of biotin. One method to investigate this dynamic behavior is with temperature dependence studies, which has become an

important tool for elucidating the mechanism of catalysis and the linkage between catalysis and conformational changes.

1.4 Temperature Dependence Studies. Structural studies of enzymes have influenced our view of catalysis enormously by providing three-dimensional representations of active sites. However, whereas these time-averaged structures are extremely useful for evaluating and modeling catalysis, they lack the ability to incorporate the dynamic motion that can occur in proteins and its effect on activity. Thus, investigations into whether protein dynamics have an effect on the catalysis of bond formation is receiving considerable attention.

From the earliest study of reaction rates, it has been evident that catalysis is strongly influenced by temperature. Thus, temperature must always be controlled if useful results are to be obtained from kinetic experiments. However, by carrying out measurements at several temperatures, one can deduce important information about reaction mechanisms.

Cornish-Bowden (1995) cites that studies by van't Hoff in 1884 and Arrhenius in 1889 into the thermodynamics of temperature on enzymatic reactions now form the basis for all modern theories of temperature dependence of rate constants. In 1867, Harcourt had noted that the rates of many reactions approximately doubled for each 10°C rise in temperature, but van't Hoff and Arrhenius attempted to find a more precise relationship by comparing kinetic observations with the known properties of equilibrium constants. van't Hoff showed that any equilibrium constant K varies with absolute temperature T in accordance with the van't Hoff equation

$$d \ln K/dT = \Delta H°/RT^2 \qquad (1.1)$$

where R is the gas constant and ΔH° is the standard change of enthalpy for the reaction. In analogy to this relationship, Arrhenius expressed the temperature dependence of the rate constant *k* by

$$d \ln k/dT = - E_a/RT^2 \quad (1.2)$$

in which E_a is the activation energy and corresponds to the standard enthalpy of reaction ΔH° in the van't Hoff equation. Then, by a separation of variables,

$$d \ln k = (-E_a/R)(dT/T^2) \quad (1.3)$$

This expression can be integrated to give

$$\ln k = -E_a/RT + \ln A \quad (1.4)$$

The frequency factor, *A,* may be thought of as the frequency of collisions with the proper orientation to produce a chemical reaction. This factor can be as large as $10^{13}sec^{-1}$, which is about the frequency of collisions of molecules in liquids. This form of the Arrhenius equation is the most convenient for graphical purposes, as it shows that a plot of ln *k* against 1/T is a straight line with of slope $-E_a/R$. This plot, known as an Arrhenius plot, provides a simple method of evaluating E_a.

After taking the exponential of both sides we get the Arrhenius equation

$$k = A \exp (-E_a/RT) \quad (1.5)$$

According to Boltzmann's theory of the distribution of energies among molecules, the number of molecules in a mixture that have energies in excess of E_a is proportional to exp $(-E_a/RT)$. We can interpret the Arrhenius equation to mean that molecules can take part in a reaction only if their energy exceeds some threshold value, the activation energy.

For the forward reaction of reactants to products, E_a is the difference in energy between the transition state and the reactants. The factor exp ($-E_a/RT$) represents the fraction of reagent molecules having the critical energy E_a for the reaction to occur.

In relating rate constants with the transition-state of a reaction, Eyring (1935) published his transition-state theory, which is still the most widely used conceptual scheme for discussing reaction rates. The central idea of this theory is that at any given temperature, the rate of reaction depends only on the concentration of the high-energy activated complex which is in equilibrium with the reactants. As a reaction is progressing, it must pass through a maximum energy state, which is known as the transition state. All properties of the activated complex are denoted with a double dagger, ‡. A bimolecular reaction can be represented by

$$E + S \underset{}{\overset{K^{\ddagger}}{\rightleftharpoons}} ES^{\ddagger} \longrightarrow E + P$$

where $ES^{\ddagger}$, the enzyme-substrate complex, is the transition state. Its concentration is assumed to be governed by the laws of thermodynamics, so that $[ES^{\ddagger}] = K^{\ddagger}[E][S]$, where $K^{\ddagger}$ is given by

$$\Delta G^{\ddagger} = -RT \ln K^{\ddagger} = \Delta H^{\ddagger} - T\Delta S^{\ddagger} \qquad (1.6)$$

where $\Delta G^{\ddagger}$, $\Delta H^{\ddagger}$, and $\Delta S^{\ddagger}$ are the Gibbs energy, enthalpy and entropy of formation, respectively, of the transition state from the reactants. Therefore, the concentration of $ES^{\ddagger}$ can be determined by

$$[ES^{\ddagger}] = [E][S]\, e^{\Delta S^{\ddagger}/R}\, e^{-\Delta H^{\ddagger}/RT} \qquad (1.7)$$

To introduce time and the rate constant for the breakdown of ES, we need to use the second-order rate constant for the complete reaction, as denoted by

$$k = RT/N_A h \, e^{\Delta S^{\ddagger}/R} \, e^{-\Delta H^{\ddagger}/RT} \tag{1.8}$$

where N_A is Avogadro's number and h is Planck's constant.

Taking the natural log of 1.8, we get

$$\ln k = \ln (RT/N_A h) + \Delta S^{\ddagger}/R - \Delta H^{\ddagger}/RT \tag{1.9}$$

differentiating equation 1.9

$$d \ln k/dT = (\Delta H^{\ddagger} + RT)/RT^2 \tag{1.10}$$

We can relate the parameters E_a and A of the Arrhenius theory to the $\Delta H^{\ddagger}$ parameter of the Eyring theory by examining the temperature dependence of the logarithm of the rate constants in both formulations. Comparing equation 1.10 to 1.2, we see that

$$E_a = \Delta H^{\ddagger} + RT \tag{1.11}$$

The enthalpy and entropy of activation of a chemical reaction provide valuable information about the nature of the transition state, and hence about the reaction mechanism. A large enthalpy of activation ($\Delta H^{\ddagger}$) indicates that a large amount of stretching or breaking of chemical bonds is necessary for the formation of the transition state (Cornish-Bowden, 1995).

The entropy of activation gives a measure of the inherent probability of the transition state, apart from energetic considerations. If $\Delta S^{\ddagger}$ is large and negative, the formation of the transition state requires the reacting molecules to orient into conformations and approach each other at a precise angle. As molecules vary widely in their conformational

stability (i.e. their rigidity and complexity) one might expect that the values of $\Delta S^{\ddagger}$ would vary widely between different reactions, which does, in fact, occur.

1.5 Solvent Isotope Effects. Tipton and Cleland (1988) observed an inverse solvent isotope effect in the reaction catalyzed by biotin carboxylase, which suggested a sulfhydryl group abstracts the proton from the 1′ nitrogen of biotin and hypothesized that the resulting enol tautomer of biotin attacks the CO_2 from the carboxyphosphate intermediate, forming carboxybiotin. Work conducted by Levert *et al.* (2000) confirmed the inverse solvent isotope effect by *E. coli* biotin carboxylase on both V_m and V/K parameters. However, their work demonstrated that a sulfhydryl did not remove the proton from 1′ nitrogen of biotin and that the origin of the kinetic solvent isotope effect remains unknown.

We examined the temperature dependence of the kinetic isotope effect to gain insight into the following questions. First, is the kinetic solvent isotope effect associated with a conformational change, or is it involved in a change in the rate-determining step? Second, is the rate-determining step affected by temperature? Third, does proton transfer in biotin carboxylase involve tunneling, the phenomenon by which a proton transfers through a reaction barrier (as opposed to over it) as a result of its wave-like property?

CHAPTER 2

MATERIALS AND METHODS

2.1 Materials. HEPES (N- [2-hydroxyethyl] piperazine-N′ -[2-ethanesulfonic acid]), lactate dehydrogenase, ATP, NADH, phosphoenolpyruvate, D_2O and ampicillin were purchased through Sigma. Pyruvate kinase was purchased through Roche. Potassium bicarbonate was purchased through EM Science. $MgCl_2$ was purchased through Mallinckrodt. Biotin was purchased through Amresco. His-binding resin was purchased through Novagen. KCl was purchased through Fisher. Isopropyl-β-D-thiogalactopyranoside (IPTG) was purchased through Research Products International.

2.2 Growth Conditions for the Overexpression of Biotin Carboxylase. Plasmid pGLW2 coding for wild type biotin carboxylase that was transformed into *E. coli* BL21 (DE3) pLysS was streaked onto an LB agar plate containing 50 ug/ml of ampicillin. A single colony was transferred to a 2L flask containing 1L of LB media and 50 ug/ml of ampicillin. The cultures were grown at 37°C at 250 rpm in a Model G25 Incubator Shaker (New Brunswick Scientific, Edison, NJ) until the A_{600} reached 0.4 – 0.6, then IPTG was added to a final concentration of 0.2 mM. After induction, the cells were grown until saturation (~ 8 hrs) and harvested by centrifugation at 8,000 X g for 10 min at 4°C. Cell paste from 1L of culture was suspended in 37.5 ml of binding buffer (50 mM imidazole, 500 mM NaCl, 20 mM Tris, pH 7.9) and frozen at -20°C until use.

2.3 Purification. Cell paste was thawed and 0.3 ug/ml of DNase and 0.37g $MgCl_2$ were added and the cell suspension was sonicated in a Branson Sonifier 250 (VWR Scientific)

for 6 min. The cell lysate was stirred for an additional 5 minutes and centrifuged at 20,000 X g for 1 hour to remove cell debris. The supernatant was collected and 0.17g of Triton X-100 was added to 160 ml of supernatant. The supernantant was loaded onto 2.5 ml columns of His-binding resin that were equilibrated in 12.5 ml of binding buffer for nickel affinity chromatography. Biotin carboxylase was eluted from the columns with 170 mM imidazole, 500 mM NaCl, 20 mM Tris, pH 7.9. The protein solution was dialyzed overnight against 2L binding buffer and the nickel affinity chromatography procedure was repeated. After the second nickel affinity chromatography, the protein solution was dialyzed in 2L phosphate buffer (10 mM KH_2PO_4, 50 mM NaCl, pH 7.1) for 3.5 hrs to prevent total precipitation of biotin carboxylase. The protein solution was then loaded onto a DEAE-cellulose column (DE-52, Whatman) equilibrated in phosphate buffer, collected immediately, and the column was washed with 35 ml of phosphate buffer to remove all the biotin carboxylase from the column. Protein was precipitated with 60% ammonium sulfate. The precipitate was centrifuged at 12,000 X g for 20 min and the pellet was resuspended in a minimal volume of dialysis buffer (500 mM KCl, 10 mM HEPES, pH7.0) and dialyzed overnight in the same buffer. Biotin carboxylase was concentrated using a colloidal membrane (Schleicher & Schuell, MWCO 25,000). Protein concentrations were determined using the Bradford assay with BSA as a standard.

2.4 Enzyme Assays. A continuous spectrophotometric assay was used to measure the activity of biotin carboxylase at different temperatures. The production of ADP was coupled to pyruvate kinase and lactate dehydrogenase, and the oxidation of NADH was followed at 340 nm. Each reaction was carried out in a volume of 0.5 ml in 1 cm path

length quartz cuvettes. The reaction mixture for H_2O contained 31.3 units/ml of pyruvate kinase, 29.6 units/ml of lactate dehydrogenase, 2 mM phosphoenolpyruvate, 0.2 mM NADH, 8 mM $MgCl_2$, 1 mM ATP, 5 mM $KHCO_3$, and 100 mM HEPES at pH 8.0. The reaction mixture for D_2O contained 31.3 units/ml of pyruvate kinase, 53.3 units/ml of lactate dehydrogenase, 2 mM phosphoenolpyruvate, 0.2 mM NADH, 8 mM $MgCl_2$, 1 mM ATP, 5 mM $KHCO_3$, and 100 mM HEPES at pD 8.0 (pD = pH + 0.4). Since we focused on temperature dependence, care was taken with the control of pH (or pD), adjusting the pH (or pD) of buffers and solutions to each temperature utilizing the Henderson-Hasselbach equation to correct for the temperature effect on the ionization of reaction components. Prior to the assays in H_2O and D_2O, controls were conducted at the high temperature (50°C) to ensure that the coupling enzymes were saturated and not rate limiting. Because the K_m for biotin is high (100 mM), the ionic strength of the reaction mixture was held constant with KCl when the initial velocity was measured as a function of biotin concentration. Values of V_m and V/K were calculated per active site using a value of 50,000 for the molecular mass of the monomer of biotin carboxylase, which exists as a homodimer.

Data were collected using a Uvikon 810 (Kontron Instruments) spectrophotometer interfaced with a PC equipped with a data acquisition program. Reactions were initiated by the addition of enzyme. The spectrophotometer temperature was maintained at assay temperature using a Lauda RM 6 RMT circulating water bath (Brinkmann). All components of the reaction mixture were pre-incubated at the assay temperature for the same length of time as the assay in a Lauda RM 6 circulating water bath (Brinkmann).

Reaction cuvettes were pre-incubated at temperature inside the spectrophotometer for twice the length of the assay time and removed for <1 min to allow for loading of the reaction before placing back into the spectrophotometer. All temperatures were confirmed with a digital probe thermometer and the error was no more than ±0.1°C.

2.5 Data Analysis.

2.5.1 van't Hoff Plot. The van't Hoff plot was used to determine the ΔH° for the binding of biotin to the enzyme-ATP-bicarbonate complex. The data were fitted by linear regression to the following equation

$$-\ln K_m = \Delta H°/RT$$

where K_m is Michaelis constant for biotin, ΔH° is the standard change in enthalpy, R is the gas constant (1.98×10^{-3} kcal/mol · K), and T is the absolute temperature in Kelvin. The slope of the van't Hoff plot is equal to ΔH°/R.

The standard free-energy change, ΔG°, for the binding of biotin to the enzyme-ATP-bicarbonate complex was calculated using the following equation

$$\Delta G° = - RT \ln K_m$$

Using the ΔG° and ΔH°, the change in entropy, ΔS°, was calculated for each temperature using the following equation

$$\Delta G° = \Delta H° - T\Delta S°$$

2.5.2 Arrhenius Plot. The Arrhenius plot was used to determine the E_a, the activation energy of the reaction. The data were fitted by linear regression to the following equation

$$\ln V_m = -E_a/RT + \ln A$$

where V_m is the maximal velocity at a given temperature, E_a is the activation energy, R is the gas constant, T is the absolute temperature, and *A* is frequency of collisions. The slope of the Arrhenius plot is equal to $-E_a/R$.

The activation enthalpy, $\Delta H^{\ddagger}$, for the reaction was calculated using the following equation

$$\Delta H^{\ddagger} = E_a - RT$$

where E_a is the activation energy, R is the gas constant and T is the absolute temperature. The free energy change of activation, $\Delta G^{\ddagger}$, for the reaction was calculated using the following equation

$$\Delta G^{\ddagger} = -RT \ln (V_m h/k_B T)$$

where V_m is the maximal velocity at a given temperature, *h* is Planck's constant (3.974×10^{-25} erg/min) and k_B is the Boltzmann constant (1.38×10^{-16} erg/deg, the gas constant per molecule).

Using $\Delta G^{\ddagger}$ and $\Delta H^{\ddagger}$, the activation entropy, $\Delta S^{\ddagger}$, was calculated for each temperature using the following equation

$$\Delta G^{\ddagger} = \Delta H^{\ddagger} - T\Delta S^{\ddagger}$$

The frequency of collisions, *A*, was calculated at each temperature using the following equation

$$\ln V_m = \ln A - E_a/RT$$

2.5.3 Eyring Plot. To determine the $\Delta H^{\ddagger}$ directly, an Eyring plot was used. The data were fitted by linear regression to the following equation

$$\ln V_m/T = -\Delta H^{\ddagger}/RT$$

where V_m is the maximal velocity, T is the absolute temperature, $\Delta H^{\ddagger}$ is the activation enthalpy, and R is the gas constant. The slope of the Eyring plot is equal to $-\Delta H^{\ddagger}/R$.

CHAPTER 3

RESULTS

3.1 Temperature Dependent Kinetics in H_2O.

3.1.1 Kinetic Parameters. The activity of biotin carboxylase increased with increasing temperature. The temperature variation for V_m is shown in Figure 1. The V_m increased 10-fold from the minimal temperature (5°C) to the maximal temperature (50°C) and almost 2-fold from physiological temperature to 50°C. The Michaelis constant, K_m, also showed a similar trend but with only a 2-fold increase from the minimal to maximal temperature with no significant increase at any given temperature as seen with V_m values (Figure 2). The correlation coefficient for the plot of K_m versus temperature was 0.93. As with the first order rate constant, V_m, the second order rate constant, V/K, showed a similar rate of increase, with the values increasing 5-fold from minimal to maximal temperature (Figure 3). The kinetic parameters for each temperature are listed in Table 1.

3.1.2 van't Hoff Plot. The temperature variation of the equilibrium constant for the binding of biotin to the biotin carboxylase-ATP-bicarbonate complex was analyzed with a van't Hoff plot, shown in Figure 4. The data were fitted to equation 1.1 to determine the change in enthalpy, $\Delta H°$, of the binding of biotin to the biotin carboxylase-ATP-bicarbonate complex. The K_m for biotin can be used as an apparent binding constant. Assuming that the on-rate constant is diffusion limited at $10^9 \cdot M^{-1} \cdot s^{-1}$ and using the K_m at 25°C of 111.5 mM (Table 1), the calculated off-rate constant is 1.12×10^8 compared to a forward catalytic rate of 1.12 sec^{-1}. Thus, the off-rate constant is 10^8 greater than the

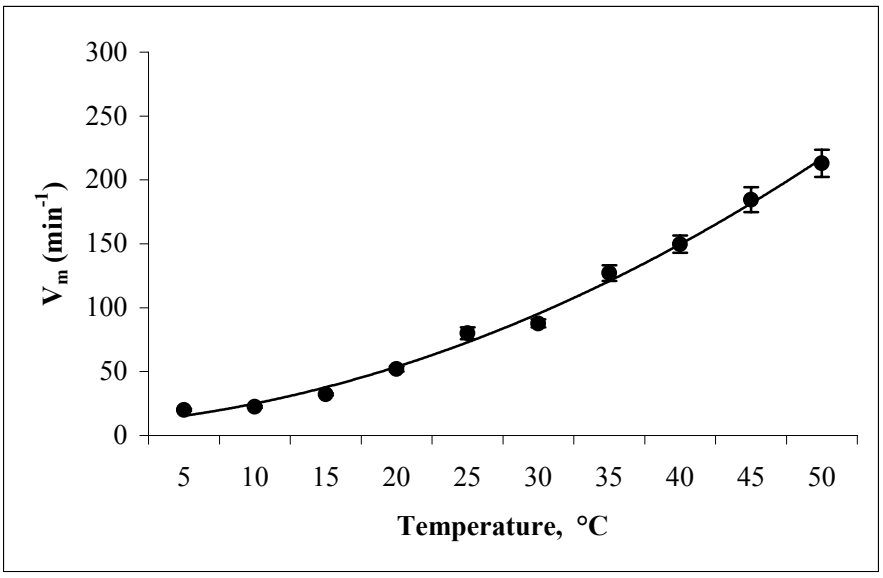

Figure. 1. Effect of temperature on maximal velocity, V_m, for the carboxylation reaction of biotin carboxylase in H_2O.

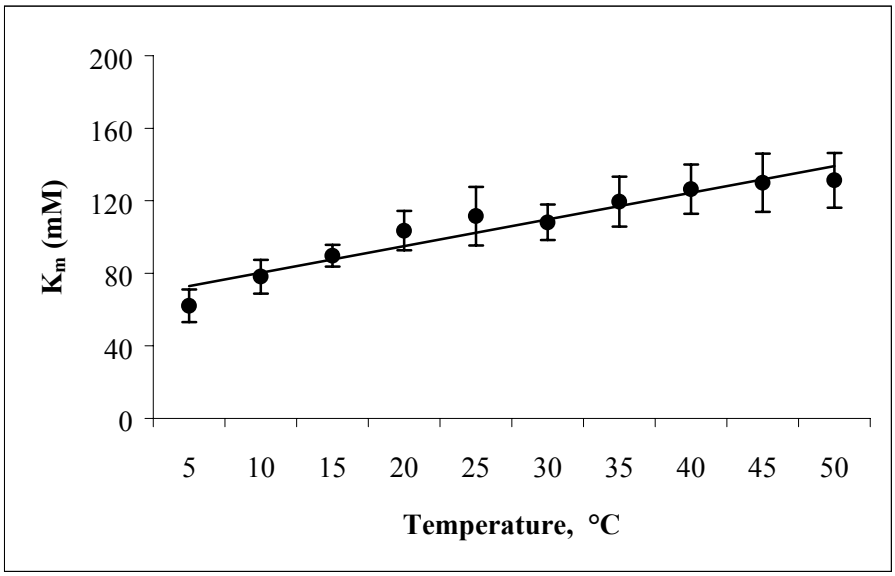

Figure 2. Effect of temperature on the Michaelis constant, K_m, for the carboxylation reaction of biotin carboxylase in H_2O.

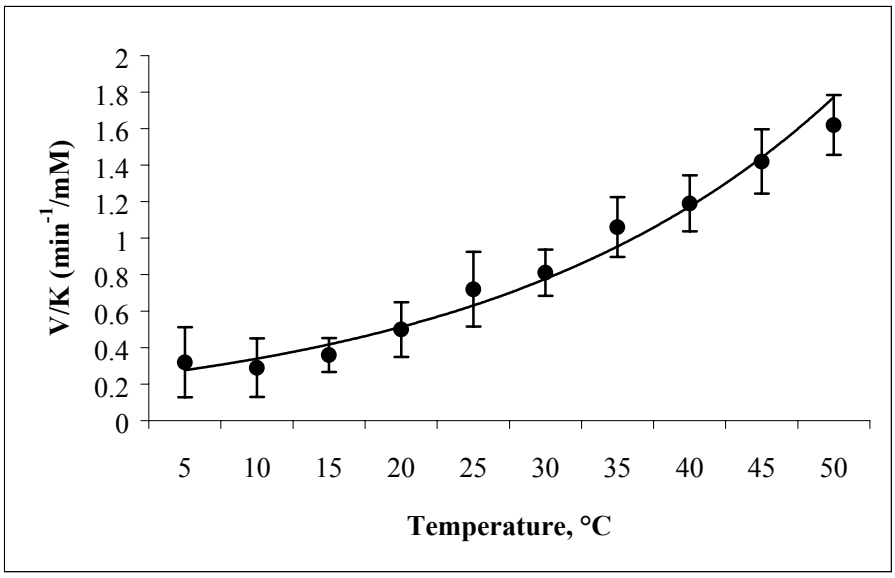

Figure 3. Effect of temperature on the second-order rate constant, V/K, for the carboxylation reaction of biotin carboxylase in H_2O.

Table 1. Kinetic Parameters of the Temperature Dependent Carboxylation of Biotin in H_2O[a]

T (K)	V_m (min^{-1})	K_m (mM)	V/K (min^{-1}/mM)
278	20.13 ± 0.96	62.15 ± 9.02	0.32 ± 0.03
283	22.42 ± 0.96	78.17 ± 9.26	0.29 ± 0.02
288	32.20 ± 0.79	89.68 ± 6.06	0.36 ± 0.02
293	52.09 ± 2.11	103.5 ± 10.8	0.50 ± 0.03
298	80.09 ± 4.63	111.5 ± 16.1	0.72 ± 0.07
303	87.67 ± 3.13	108.1 ± 9.8	0.81 ± 0.05
308	127.1 ± 6.1	119.5 ± 13.8	1.06 ± 0.08
313	149.8 ± 6.8	126.4 ± 13.6	1.19 ± 0.08
318	184.5 ± 9.8	129.9 ± 16.1	1.42 ± 0.11
323	213.0 ± 10.5	131.3 ± 15.1	1.62 ± 0.11

[a]The kinetic parameters were determined by varying [biotin] at constant saturating levels of bicarbonate and ATP. The standard errors on V_m and K_m were determined by nonlinear regression analysis. The error on V/K was calculated by standard propagation of the errors from V_m and K_m.

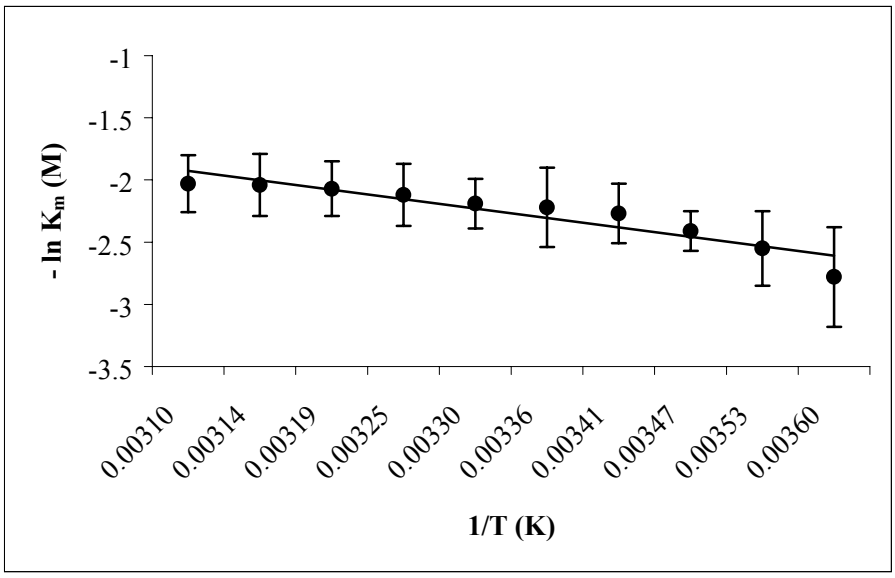

Figure 4. van't Hoff plot showing the relationship between the equilibrium constant, K_m, and temperature in H_2O. $\Delta H°$ is derived from the slope $\Delta H°/R$. The points are experimental values and the line represents the best-fit line to equation 1.1.

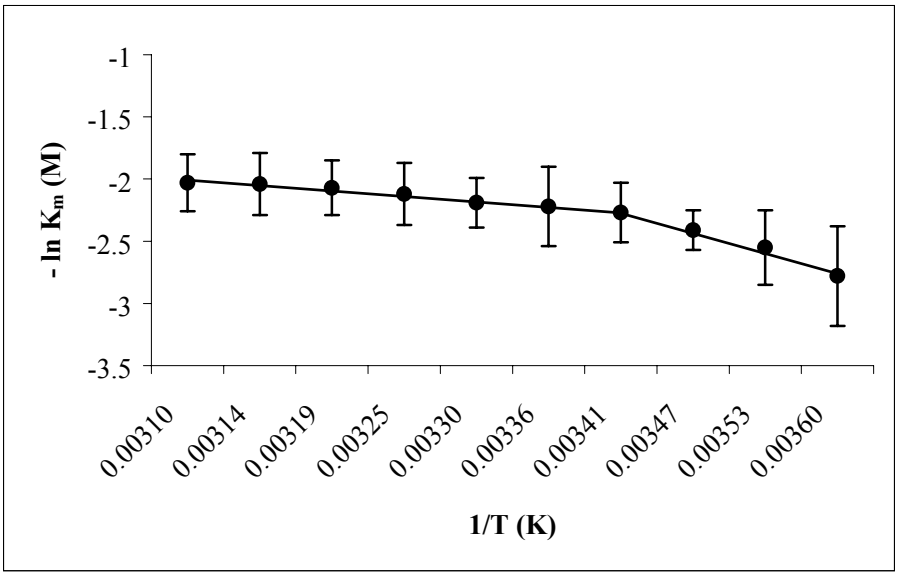

Figure 5. van't Hoff plot where 5-20°C and 20-50°C were fitted, respectively, to equation 1.1.

on-rate constant, therefore the complex is in equilibrium. The $\Delta H°$ was calculated to be -2.74 ± 0.32 kcal/mol. However, after analysis of the residuals, the data showed a systematic error (Appendix, Figure 16). Therefore, the data were divided into two regions (Figure 5). The first region consisted of values from 5-20°C, which gave a $\Delta H°$ of -4.55 ± 1.84 kcal/mol, and a second region, 20-50°C, which gave a $\Delta H°$ of -1.59 ± 0.16 kcal/mol.

3.1.3 Arrhenius Plot. The temperature variation of the maximal velocity was analyzed with an Arrhenius plot, shown in Figure 6. The data were fitted to equation 1.2 to determine the activation energy, E_a, of the reaction. E_a is the difference in energy between the transition state and the reactants. The slope gave an E_a value of 10.09 ± 0.48 kcal/mol. The frequency of collisions, *A*, for each temperature in H_2O was determined from E_a and equation 1.4 (Table 2). Interestingly, the *A* for the reaction at 25°C had the greatest value, 3.36 (± 0.04) x $10^7 \cdot sec^{-1}$, with an apparent decrease at higher and lower temperatures, respectively. So, according to the Arrhenius theory, the maximal velocity is determined by the ratio of activation energy to the temperature and by the frequency of collisions that produce a reaction.

3.1.4 Eyring Plot. The E_a from the Arrhenius plot was then related to the quasi-thermodynamic quantities of the Eyring plot by analyzing the temperature dependence of the maximal velocity at a specific temperature using equation 1.11 to determine the enthalpy of activation, $\Delta H^{\ddagger}$. $\Delta H^{\ddagger}$ differs from $\Delta H°$, derived from the van't Hoff plot, in that it refers to the transition state of a reaction. The $\Delta H^{\ddagger}$ calculated from the linear fit

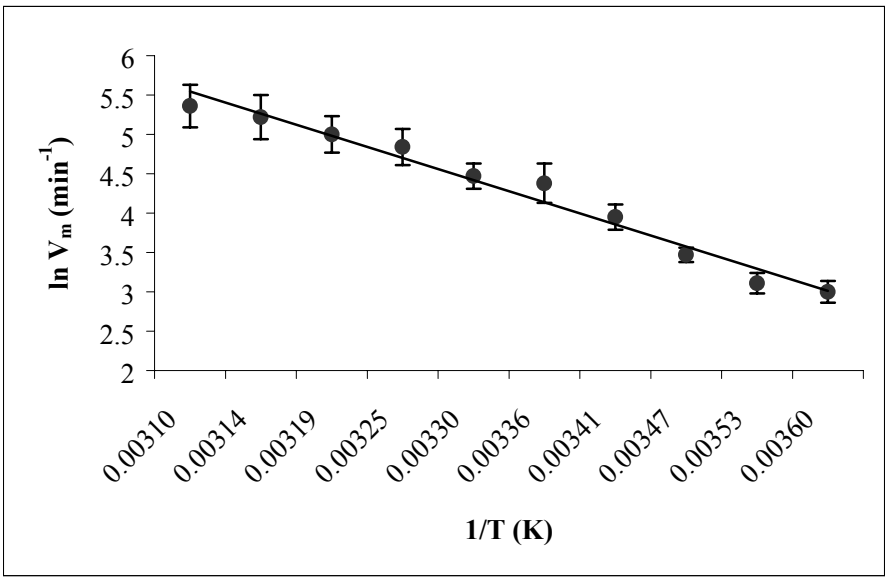

Figure 6. Arrhenius plot showing the relationship between the maximal velocity, V_m, and temperature in H_2O. E_a is derived from the slope – E_a/R. The points are experimental values and the line represents the best-fit line to equation 1.2.

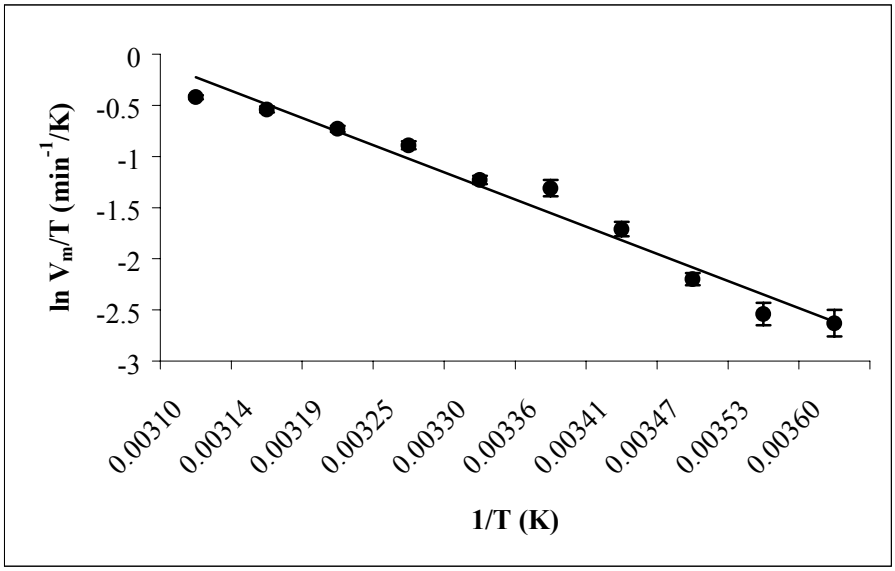

Figure 7. Eyring plot showing the relationship between the temperature dependence of the maximal velocity, V_m, and temperature in H_2O. $\Delta H^{\ddagger}$ is derived from the slope - $\Delta H^{\ddagger}/R$. The points are experimental values and the line represents the best-fit line to equation 1.10.

Table 2. Thermodynamic Parameters of the Temperature Dependent Carboxylation of Biotin in H_2O

T (K)	$\Delta G^{\circ a}$ (kcal/mol)	$\Delta H^{\circ b}$ (kcal/mol)	$\Delta S^{\circ c}$ (cal/mol)
278	1.54 ± 0.22	-4.55 ± 1.84	-21.9 ± 5.8
283	1.43 ± 0.17	-4.55 ± 1.84	-21.1 ± 5.9
288	1.38 ± 0.09	-4.55 ± 1.84	-20.6 ± 6.0
293	1.32 ± 0.14	-4.55 ± 1.84/-1.59 ± 0.16	-20.0 ± 5.8/-9.93 ± 0.16
298	1.30 ± 0.19	-1.59 ± 0.16	-9.70 ± 0.10
303	1.34 ± 0.12	-1.59 ± 0.16	-9.67 ± 0.13
308	1.30 ± 0.15	-1.59 ± 0.16	-9.38 ± 0.03
313	1.29 ± 0.14	-1.59 ± 0.16	-9.20 ± 0.16
318	1.29 ± 0.16	-1.59 ± 0.16	-9.06
323	1.30 ± 0.15	-1.59 ± 0.16	-8.95 ± 0.03

T (K)	$\Delta G^{\ddagger d}$ (kcal/mol)	$\Delta H^{\ddagger e}$ (kcal/mol)	$\Delta S^{\ddagger f}$ (cal/mol)	A^g (sec^{-1})
278	12.27 ± 0.59	9.45 ± 0.45	-10.1 ± 0.5	2.91 (± 0.12) x 10^7
283	12.44 ± 0.53	9.46 ± 0.45	-10.5 ± 0.3	2.31 (± 0.09) x 10^7
288	12.46 ± 0.31	9.47 ± 0.45	-10.4 ± 0.5	2.44 (± 0.05) x 10^7
293	12.41 ± 0.51	9.48 ± 0.46	-10.0 ± 0.2	2.92 (± 0.02) x10^7
298	12.38 ± 0.72	9.49 ± 0.46	-9.7 ± 0.9	3.36 (± 0.04) x 10^7
303	12.54 ± 0.45	9.50 ± 0.46	-10.03 ± 0.03	2.78 (± 0.02) x 10^7
308	12.53 ± 0.60	9.51 ± 0.46	-9.8 ± 0.5	3.06 (± 0.09) x 10^7
313	12.64 ± 0.58	9.52 ± 0.46	-10.0 ± 0.4	2.79 (± 0.09) x 10^7
318	12.73 ± 0.67	9.53 ± 0.46	-10.1 ± 0.7	2.64 (± 0.13) x 10^7
323	12.84 ± 0.64	9.54 ± 0.46	-10.2 ± 0.6	2.39 (± 0.13) x 10^7

[a, d] ΔG° and $\Delta G^\ddagger$ was calculated using equation 1.6 [b, e] $\Delta H^\circ$and $\Delta H^\ddagger$ was calculated using equation 1.11. [c, f] $\Delta S^\circ$and $\Delta S^\ddagger$ was calculated with equation 1.6. [g] *A* was calculated using equation 1.4.

of all the data in the Eyring Plot (Figure 7) was 9.52 ± 0.5 kcal/mol. The $\Delta H^\ddagger$ for each temperature determined from equation 1.11, in addition to the thermodynamic parameters of the activation energy, $\Delta G^\ddagger$, and the activation entropy, $\Delta S^\ddagger$, (determined from equations 1.17 and 1.18) are listed in Table 2.

3.2 Temperature Dependent Kinetics in D_2O.

3.2.1 Kinetic Parameters. The activity of biotin carboxylase in 80% D_2O increased with increasing temperature. The temperature variation for V_m in D_2O is shown in Figure 8. The V_m increased 12-fold from the minimal temperature (5°C) to the maximal temperature (50°C) and almost 14-fold between 5-40°C, with the largest rate increase occurring between 20-25°C. The rate began to decrease at temperatures above 40°C. The second order rate constant, V/K, showed a similar rate of increase, with values increasing 9-fold between the minimal and maximal temperatures and almost 11-fold between 5-40°C. The largest increase occurred between 40-45°C (Figure 9). The kinetic parameters for each temperature in D_2O are listed in Table 3.

3.2.2 Arrhenius Plot. The temperature variation of the maximal velocity was analyzed with an Arrhenius plot, shown in Figure 10. The data were fitted to equation 1.2 to determine the activation energy, E_a, of the reaction in D_2O. The E_a was calculated to be 10.68 ± 1.22 kcal/mol. However, after analysis of the residuals, the data showed a systematic error (Appendix, Figure 17). Therefore, the data were divided into two regions (Figure 11). The first region, corresponding to values from 5-25°C, gave an E_a of 16.35 ± 0.90 kcal/mol, and a second region, 25-50°C, which gave an E_a of 4.01 ± 1.15 kcal/mol.

The frequency of collisions, *A*, for each temperature in D_2O was determined from the Ea and equation 1.4 (Table 4). Again, the *A* for the reaction at 25°C had the greatest value, $1.72 \times 10^{12} \cdot sec^{-1}$, with a slight decrease at lower temperatures and a sharp decrease at higher temperatures, respectively.

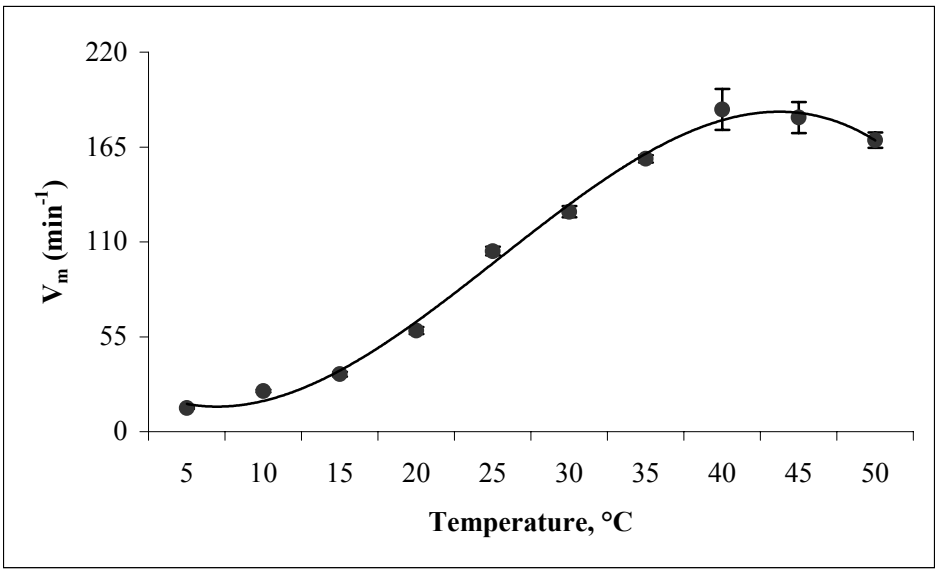

Figure 8. Effect of temperature on maximal velocity, V_m, for the carboxylation reaction of biotin carboxylase in D_2O.

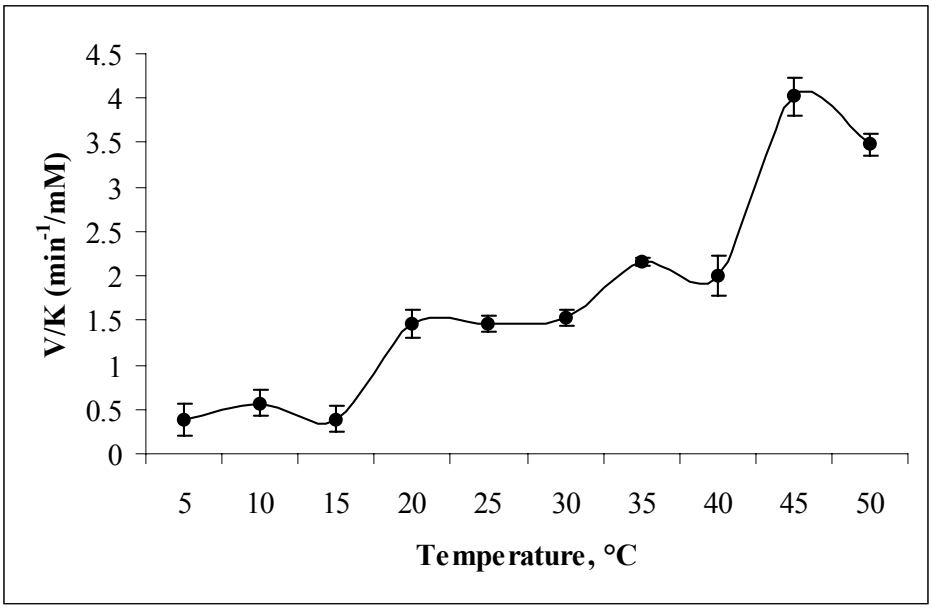

Figure 9. Effect of temperature on the second-order rate constant, V/K, for the carboxylation reaction of biotin carboxylase in D_2O.

Table 3. Kinetic Parameters of the Temperature Dependent Carboxylation of Biotin in D_2O[a].

T (K)	V_m (min^{-1})	K_m (mM)	V/K (min^{-1}/mM)
278	13.68 ± 0.55	35.7 ± 5.0	0.38 ± 0.18
283	23.55 ± 0.74	41.4 ± 4.5	0.57 ± 0.14
288	33.3 ± 1.4	85.8 ± 8.7	0.39 ± 0.14
293	58.56 ± 2.02	40.0 ± 5.1	1.46 ± 0.16
298	104.7 ± 2.5	71.1 ± 4.7	1.47 ± 0.09
303	127.5 ± 3.3	82.8 ± 5.3	1.54 ± 0.09
308	158.2 ± 2.2	73.1 ± 2.8	2.16 ± 0.05
313	186.8 ± 11.9	92.7 ± 15.1	2.01 ± 0.23
318	182.1 ± 9.0	45.3 ± 7.5	4.02 ± 0.22
323	169 ± 4.5	48.5 ± 4.6	3.48 ± 0.12

[a]The kinetic parameters were determined by varying [biotin] at constant saturating levels of bicarbonate and ATP. The standard errors on V_m and K_m were determined by nonlinear regression analysis.

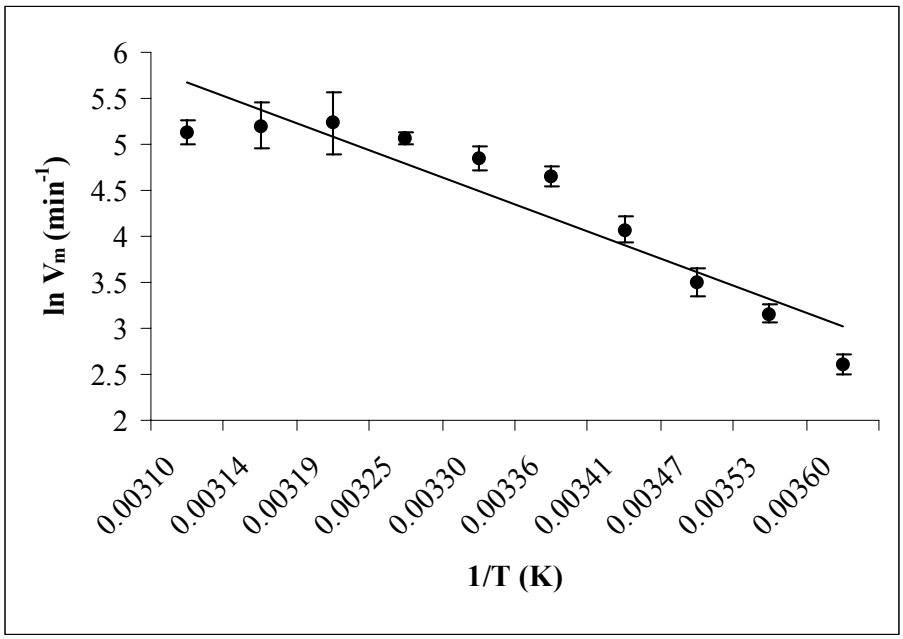

Figure 10. Arrhenius plot showing the relationship between the maximal velocity,V_m, and temperature in D_2O. E_a is derived from the slope – E_a/R. The points are experimental values and the line represents the best-fit line to equation 1.2.

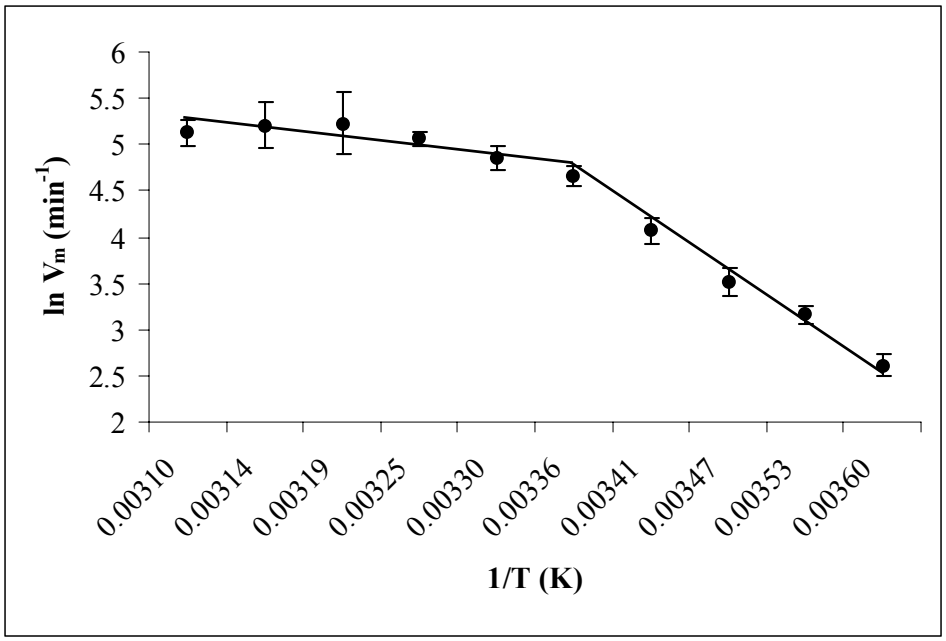

Figure 11. Arrhenius plot where 5-25°C and 25-50°C were fitted, respectively, to equation 1.2.

Table 4. Thermodynamic Parameters of the Temperature Dependent Carboxylation of Biotin in D_2O

T (K)	$\Delta G^{\ddagger a}$ (kcal/mol)	$\Delta H^{\ddagger b}$ (kcal/mol)	$\Delta S^{\ddagger c}$ (cal/mol)	$A^{d, e}$ (sec^{-1})
278	12.5 ± 0.5	15.8 ± 0.9	11.8 ± 0.1	1.66×10^{12}
283	12.5 ± 0.4	15.8 ± 0.9	11.8 ± 0.1	1.66×10^{12}
288	12.5 ± 0.5	15.8 ± 0.9	11.4 ± 0.1	1.45×10^{12}
293	12.4 ± 0.4	15.8 ± 0.9	11.5 ± 0.9	1.54×10^{12}
298	12.3 ± 0.3	15.8 ± 0.9/3.4 ± 1.0	11.1 ± 0.1/-29.7 ± 0.3	1.72×10^{12}/1.53 (± 0.32) x 10^3
303	12.4 ± 0.3	3.4 ± 1.0	-29.5 ± 0.3	1.67 (± 0.14) x 10^3
308	12.4 ± 0.2	3.4 ± 1.0	-29.3 ± 0.3	1.85 (± 0.07) x 10^3
313	12.6 ± 0.8	3.4 ± 1.0	-29.3 ± 0.4	1.95 (± 0.44) x 10^3
318	12.8 ± 0.6	3.4 ± 1.0	-29.6 ± 0.3	1.73 (± 0.30) x 10^3
323	13.0 ± 0.4	3.4 ± 1.0	-29.9 ± 0.3	1.46 (± 0.18) x10^3

[a]$\Delta G^{\ddagger}$ was calculated using equation 1.6 [b]$\Delta H^{\ddagger}$ was calculated using equation 1.11. [c]$\Delta S^{\ddagger}$ was calculated with equation 1.6. [d]*A* was calculated using equation 1.4.[e]Errors not indicated due to small value. Two values indicate a transition temperature and the calculations for each value are shown.

3.2.3 Eyring Plot. The temperature dependence of the maximal velocity as a function of temperature was analyzed using equation 1.11 to determine the enthalpy of activation, $\Delta H^{\ddagger}$. The $\Delta H^{\ddagger}$ calculated from the linear fit of all the data in the Eyring plot (Figure 12) was 10.06 ± 1.22 kcal/mol. However, after examination of the residuals, the data again showed a systematic error (Appendix, Figure 18). Therefore, the data were divided into two regions (Figure 13). The first region consisted of values 5-25°C, which gave a $\Delta H^{\ddagger}$ of 15.86 ± 0.85 kcal/mol. A second region, 25-50°C, gave a $\Delta H^{\ddagger}$ of 3.37 ± 1.06 kcal/mol. The $\Delta H^{\ddagger}$ derived from Figure 13, in addition to the activation energy, $\Delta G^{\ddagger}$, and the activation entropy, $\Delta S^{\ddagger}$, (determined from equations 1.17 and 1.18) are listed in Table 4.

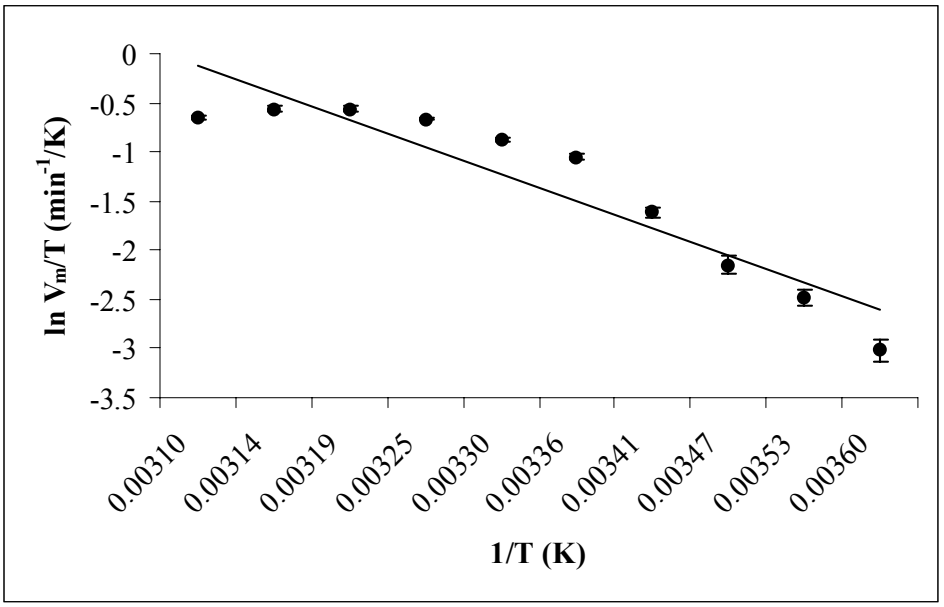

Figure 12. Eyring plot showing the relationship between the temperature dependence of the maximal velocity, V_m, and temperature in D_2O. $\Delta H^{\ddagger}$ is derived from the slope $-\Delta H^{\ddagger}/R$. The points are experimental values and the line represents the best-fit line to equation 1.10.

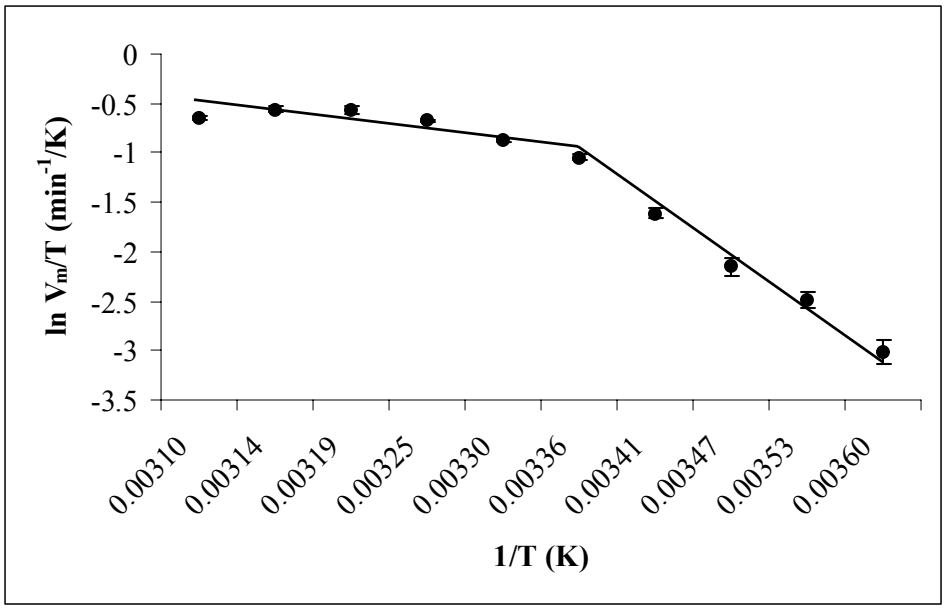

Figure 13. Eyring plot where 5-25°C and 25-50°C were fitted, respectively, to equation 1.10

3.2.4 Kinetic Solvent Isotope Effect. The $^{D}(V)$, which is the ratio of maximal velocities in H_2O and D_2O, respectively, was constant between 10-40°C. However, $^{D}(V)$ went from normal at 5°C, to inverse from 10-40°C, and back to normal at 45-50°C, showing a concave plot with the lowest value occurring at 30°C (Figure 14). A normal value corresponds to a rate that is faster in H_2O than D_2O, while an inverse value corresponds to a rate that is faster in D_2O than H_2O. The $^{D}(V/K)$, which measures the ratios of the second order rate constants in H_2O and D_2O, respectively, did not vary with temperature (Figure 15). Tipton & Cleland (1988) reported a $^{D}(V)$ at 25°C of 0.80 ± 0.02 and a $^{D}(V/K)$ of 0.50 ± 0.09. Our data for the same temperature indicates a $^{D}(V)$ of 0.76 ± 0.08 and a $^{D}(V/K)$ of 0.49 ± 0.32. Thus, the inverse kinetic solvent isotope effects of biotin

carboxylase as determined by Tipton & Cleland was confirmed. The kinetic solvent isotope effects for each temperature are listed in Table 5.

3.2.5 Hydrogen Tunneling. Analysis of the Arrhenius Preexponential factors (Table 6) show that the values are inverse at temperatures between 5-25°C, which fall below the semiclassical lower limit of 0.7 for A_H/A_D. At temperatures between 25-50°C, the A_H/A_D values are above the upper limit of the semiclassical value of 1.3. The results of these observations suggests that both hydrogen and deuterium tunneling is occurring in biotin carboxylase.

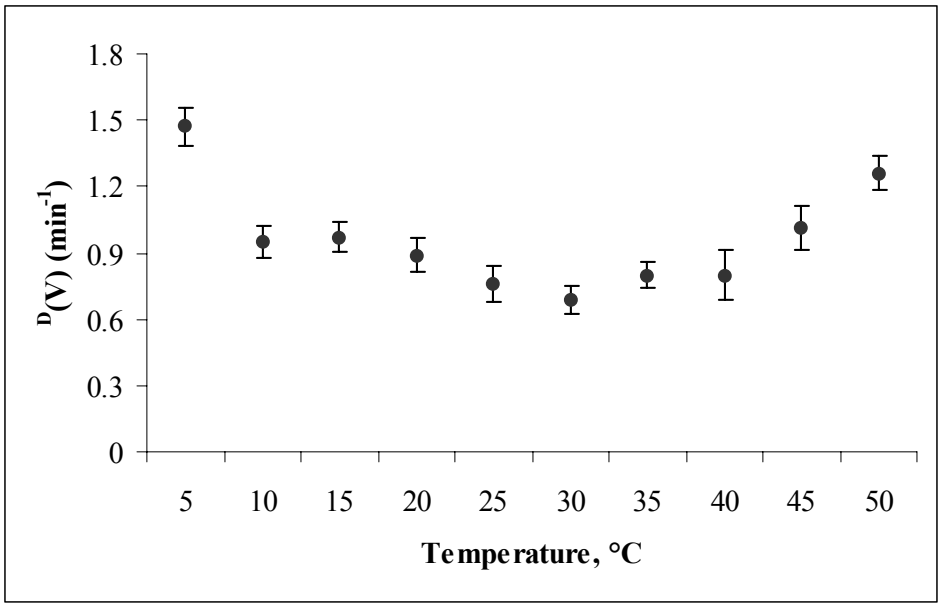

Figure 14. The ratio of first order rate constant, V_m, of H_2O and D_2O versus temperature.

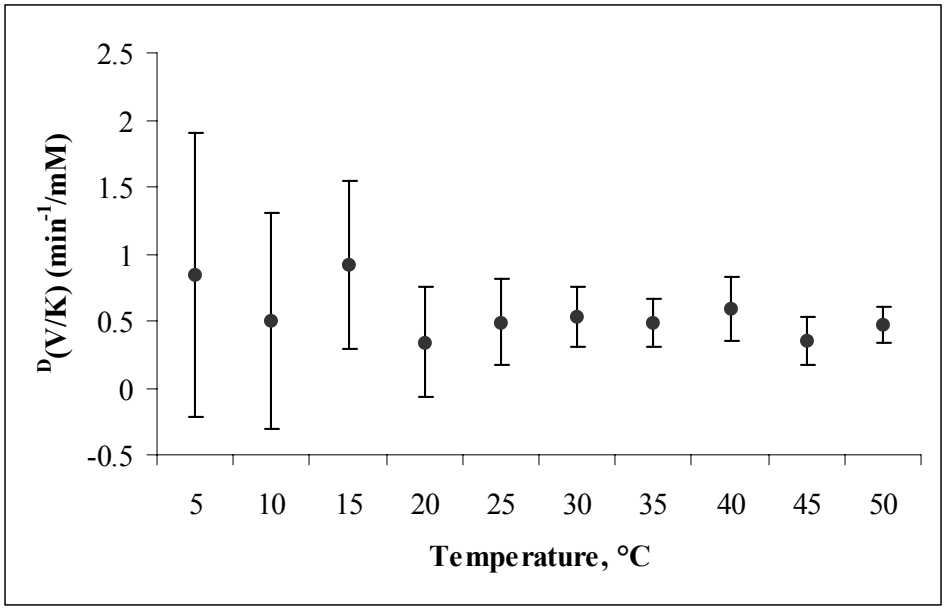

Figure 15. The ratio of the second order rate constant, V/K, of H_2O and D_2O versus temperature.

Table 5. Kinetic Solvent Isotope Effects on V_m and V/K

T (K)	$^{D}(V)$	$^{D}(V/K)$
278	1.47 ± 0.09	0.85 ± 1.06
283	0.95 ± 0.08	0.5 ± 0.8
288	0.97 ± 0.07	0.92 ± 0.63
293	0.89 ± 0.08	0.34 ± 0.41
298	0.76 ± 0.08	0.49 ± 0.32
303	0.69 ± 0.06	0.53 ± 0.22
308	0.8 ± 0.1	0.49 ± 0.18
313	0.8 ± 0.1	0.59 ± 0.24
318	1.0 ± 0.1	0.35 ± 0.18
323	1.26 ± 0.08	0.47 ± 0.14

[a]The kinetic solvent isotope effects were determined by varying biotin at constant saturating levels of bicarbonate and ATP in 80% D_2O. The error on $^{D}(V)$ and $^{D}(V/K)$ was calculated by standard propagation of the errors from V_m and K_m.

Table 6. Arrhenius Preexponential Factors[a]

T (K)	A_H	A_D[b]	A_H/A_D[b]
278	17.2 ± 2.1	28.1	0.61
283	17.0 ± 2.4	28.1	0.60
288	17.0 ± 3.0	28.0	0.61
293	17.2 ± 3.9	28.1	0.61
298	17.3 ± 3.2	28.2/7.3 ± 1.1	0.61/2.37 ± 1.18
303	17.1 ± 3.8	7.4 ± 2.0	2.31 ± 0.82
308	17.2 ± 2.4	7.5 ± 2.7	2.29 ± 0.39
313	17.1 ± 2.4	7.6 ± 0.8	2.25 ± 1.33
318	17.1 ± 2.1	7.5 ± 1.2	2.28 ± 0.77
323	17.0 ± 2.1	7.3 ± 1.7	2.33 ± 0.54

[a]The Arrhenius preexponential factors were calculated from equation 1.4. [b]Errors not indicated due to small value.

CHAPTER 4

DISCUSSION

4.1 Analysis of the van't Hoff Plot. The temperature dependence of the equilibrium constant for the binding of biotin to the biotin carboxylase-ATP-bicarbonate complex was analyzed with a van't Hoff plot. The negative value of ΔH° indicated an exothermic reaction for the binding of biotin to the biotin carboxylase-ATP-bicarbonate complex. The interpretation for the negative ΔH° value is that since K_m is an approximation of a dissociation constant, the enthalpy of the biotin carboxylase-biotin-ATP-bicarbonate complex is greater than the enthalpy of the free biotin and the biotin carboxylase-ATP-bicarbonate complex. Thus, as more heat is absorbed by the biotin carboxylase-biotin-ATP-bicarbonate complex, the thermal fluctuations increase, causing the biotin to dissociate more rapidly from the biotin carboxylase-biotin-ATP-bicarbonate complex. The ΔS° further suggests that thermal fluctuations cause the K_m to increase as a function of temperature. As temperature increases, the change in entropy is greater in biotin carboxylase-biotin-ATP-bicarbonate complex than for free biotin and free biotin carboxylase-ATP bicarbonate complex due to increasing thermal fluctuations.

The van't Hoff plot in H_2O (Figure 6) is convex, with an apparent break in the data at about 20°C. This suggests that a conformational change is occurring in biotin carboxylase at about 20°C. There are ample examples for temperature induced conformational changes in enzymes. Among these are: D-amino acid oxidase (Massey *et al*., 1966),

glutamine synthetase (Schrake *et al*., 1989), penicillopepsin (Allen *et al*., 1990), and tryptophan synthase (Fan *et al*., 2000).

4.2 Analysis of the Arrhenius and Eyring Plots in H_2O. The temperature dependence of the maximal velocity is shown in an Arrhenius plot (Figure 7), where the slope determines the energy of activation, E_a. In H_2O, the slope is linear between 5-50°C, indicating that the E_a is a constant independent of temperature (Moore, 1983). The E_a was determined from the Arrhenius plot and equation 1.11 to calculate the $\Delta H^{\ddagger}$ values at all temperatures, with the $\Delta H^{\ddagger}$ at 25°C of 9.49 ± 0.46 kcal/mol. The $\Delta H^{\ddagger}$ determined from the slope of the Eyring plot gave an overall $\Delta H^{\ddagger}$ value is 9.52 ± 0.50 kcal/mol, which compared favorably to the calculated value from the Arrhenius plot. A positive $\Delta H^{\ddagger}$ was expected because the transition state involves the breaking of bonds. The calculated $\Delta S^{\ddagger}$ was negative, indicating that the formation of the transition state requires the reacting molecules to adopt precise conformations and approach one another at a precise angle and that the molecules are more constrained in the activated complex.

The question now is: do these transition state values give us insight into the hypothesis of Sloane *et al*., (2001), who proposed a mechanism for how biotin binding to biotin carboxylase increases the rate 1100-fold? According to the hypothesis, the binding of biotin to the biotin carboxylase-ATP-bicarbonate complex preorganizes the active site to form a near attack conformer with the concurrent increase in the rate of ATP hydrolysis. A near attack conformer refers to the juxtaposition of the substrates in the ground state such that they closely resemble the transition state. Bruice and Benkovic (2000) proposed that the preorganization of the activated complex is manifested in the activation enthalpy

($\Delta H^{\ddagger}$) and not in the activation entropy ($\Delta S^{\ddagger}$). This proposal is based on numerous examples of enthalpies of activation for enzyme-catalyzed and nonenzymatic catalyzed reactions, in which the activation enthalpy varied widely between enzyme-catalyzed and nonenzymatic catalyzed reactions. In contrast, the activation entropy showed very little change between enzyme-catalyzed and nonenzymatic catalyzed reactions. Thus, it will be interesting to test this hypothesis by measuring the temperature dependence for the variety of mutant forms of biotin carboxylase that do not exhibit this 1100-fold increase in activity. If the hypothesis by Sloane *et al*. (2001) is correct, the temperature dependence will show a dramatic increase in the $\Delta H^{\ddagger}$ of the mutant enzyme with little or no change in the $\Delta S^{\ddagger}$.

However, the fact that the van't Hoff plot of the binding of biotin to the biotin carboxylase-ATP-bicarbonate complex is biphasic argues against the hypothesis of Sloane *et al* (2001). The van't Hoff plot suggests two different conformations of the enzyme, with the transition from one conformation to the other occurring at 20°C. The hypothesis of Sloane *et al*. (2001) states that the binding of biotin does not cause a conformational change in biotin carboxylase and that it preorganizes the active site. Their hypothesis was based on crystallographic data of biotin carboxylase at 4°C that showed biotin does not cause a conformational change in biotin carboxylase. However, the kinetic data for the wild type and mutants was collected at 25°C and the *in vivo* temperature is 37°C. Thus, the binding of biotin may cause a conformational change, which would result in the increased rate of ATP hydrolysis 1100-fold. Thus, the mechanism may be an induced fit and therefore involve a large conformational change.

The frequency of collisions, *A*, in H_2O was determined from E_a and equation 1.4 (Table 2). The frequency of collisions may be thought of as the frequency of collisions with the proper orientation to produce a chemical reaction. In H_2O, the frequency of collisions is relatively constant, reflecting the temperature independence of E_a.

4.3 Analysis of the Arrhenius and Eyring Plots in D_2O. In contrast to H_2O, the Arrhenius and Eyring plots in D_2O were convex. Nonlinear Arrhenius and Eyring plots indicate either a change in rate-determining step or a conformational change as a function of temperature (Fan *et al*., 2000).

To distinguish between these two possibilities, the kinetic solvent isotope effect as a function of temperature was measured for biotin carboxylase. Tipton & Cleland (1988) identified an inverse kinetic solvent isotope effect on both the V_m and V/K parameters for biotin carboxylase. Through our studies, their results at 25°C were confirmed and the kinetic solvent isotope effect was expanded through temperature dependence studies to determine whether the transition temperature was caused by a conformational change or a change in the rate-determining step. While the kinetic solvent isotope effect on the maximal velocity [^{D}(V)] was inverse between 15°C and 40°C, the isotope effect was normal at low and high temperatures, respectively, with the largest isotope effect at 30°C. The isotope effect was less inverse at 15°C and becomes normal at temperatures below 15°C. The same trend was seen at high temperatures, with the isotope effect becoming normal above 40°C. These results indicate changes in the rate-determining step as a function of temperature and are not indicative of a conformational change. However, if

the kinetic solvent isotope effect showed no change in the $^{D}(V)$, this would be indicative of a conformational change.

The frequency of collisions, *A*, was determined by using equation 1.4 (Table 4). The frequency of collisions in D_2O varies markedly above and below the transition temperature by a factor of 10^9. A plausible explanation is that at lower temperatures, which correspond to the higher *A* values (10^{12}), the active site is more rigid due to a temperature-induced effect, thus limiting the freedom of motion available at higher temperature. Hence, the frequency of collision increases. Although it would seem, by definition of the frequency of collisions, that a sufficient amount of collisions are available to produce a chemical reaction, collisions only lead to a reaction when the energy of the colliding pair exceeds the activation energy. So even though the frequency of collisions is significant at lower temperatures, they do not possess the requisite kinetic energy required to exceed the elevated E_a at lower temperatures (Moore, 1983).

4.4 Hydrogen Tunneling. Nonlinear Arrhenius plots of rate constants of the solvent isotope effects provide evidence for the tunneling in enzymatic reactions (Suhnel and Schowen, 1991). The phenomenon of tunneling results when a particle passes through an activation barrier rather than over it (Anderson, 1991). To explore this, comparison of the temperature dependence of H and D transfer were evaluated. For semiclassical hydrogen-transfer reactions, A_H/A_D is expected to be almost independent of isotopic substitution in the high temperature limit; that is, $A_H/A_D = 0.7$ to 1.3 in the absence of tunneling (Melander and Saunders, 1987). In the case of moderate amounts of tunneling, A_H/A_D is

predicted to become more inverse (i.e. < 0.7) and in the case of extreme tunneling, A_H/A_D is predicted to be greater than 1 (i.e. > 1.3) (Basran *et al*., 1999).

The Arrhenius preexponential factors for H_2O and D_2O, respectively, are given in Table 6 with the corresponding A_H/A_D values. This data shows an A_H/A_D value of ~ 2.3 above the transition temperature (25°C) and ~ 0.6 below the transition temperature. Interestingly, this data suggests that deuterium undergoes tunneling. This seems contradictory since the prediction that tunneling will occur is based in part on the mass of the particle. However, work conducted by Grant and Klinman (1989) on bovine serum amine oxidase indicated a significant amount of deuterium tunneling, which supports our findings. Further support of this hypothesis is provided by Kresge (1977) who observed that a $\Delta G°$ close to zero is a condition conducive to tunneling. Data for $\Delta G°$ in H_2O is given in Table 2; data for D_2O are not shown, but $\Delta G° < 1.9$. Thus, our data suggest that tunneling occurs in biotin carboxylase with moderate amounts of tunneling below the transition temperature to extreme tunneling above the transition temperature. Further investigation on the kinetic solvent isotope effect on mutant forms of biotin carboxylase forms will help elucidate the effect of tunneling on the rate of catalysis and identify if the effect is due to a change in the rate-determining step or a conformational change.

CHAPTER 5

CONCLUSIONS

Analysis of the temperature dependence of the carboxylation of biotin catalyzed by biotin carboxylase has allowed for the determination of the temperature dependent kinetics and thermodynamic parameters for this reaction. The kinetic parameters, not surprisingly, showed an increase in the maximal velocity, V_m, and V/K and a decrease in binding, shown with the increasing K_m values. Additionally, the data demonstrated that biotin carboxylase is stable up to 50°C.

Determination of the thermodynamic parameters was accomplished through the analysis of the van't Hoff, Arrhenius, and Eyring plots. Analysis of the Arrhenius and Eyring plots in H_2O determined the free energy of activation ($\Delta G^{\ddagger}$), activation enthalpy ($\Delta H^{\ddagger}$), and activation entropy ($\Delta S^{\ddagger}$) of ~ 12.5 kcal/mol, ~ 9.5 kcal/mol, and ~ -10.1 cal/mol, respectively (Table 2). Analysis of the thermodynamic parameters in D_2O determined $\Delta G^{\ddagger}$ to be ~ 12.5 kcal/mol, a $\Delta H^{\ddagger}$ of ~ 15.8 kcal/mol below the transition temperature and ~ 3.4 kcal/mol above the transition temperature, respectively. $\Delta S^{\ddagger}$ was ~ 11.5 cal/mol below the transition temperature and ~ -29.5 cal/mol above the transition temperature, respectively (Table 4). The free energy of activation remained fairly constant, but the activation enthalpy and entropy varied widely between H_2O and D_2O. The break in the van't Hoff plot in H_2O suggests that biotin carboxylase undergoes a temperature induced conformational change around 20°C. This result has not been previously identified for two reasons. First, crystallographic studied were done at

temperatures well below the transition temperature. Second, kinetic studies for the wild type and mutant biotin carboxylase were performed at 25°C, which is above the transition temperature. Thus, biotin may in fact cause a conformational change in biotin carboxylase through an induced fit mechanism in contrast to the proposal of preorganization of the active site occurs through the binding of ATP.

Arrhenius and Eyring plots in D_2O were nonlinear, which indicates either a change in the rate-determining step or a conformational change. Kinetic solvent isotope effects were used to distinguish between these two possibilities. The result of the kinetic solvent isotope effect suggests a change in the rate-determining step as a function of temperature is occurring and is not due to a conformational change.

An interesting finding of the kinetic solvent isotope effect was that tunneling may occur in biotin carboxylase. Analysis of Arrhenius preexponential factors (A_H/A_D) determined from the temperature dependence of the kinetic solvent isotope suggests both hydrogen and deuterium tunneling in biotin carboxylase.

REFERENCES

1. Allen, B., Blum, M., Cunningham, A., Tu, G-C., and Hofmann, T (1990) *J. Biol. Chem. 265*, 5060-5065.

2. Anderson, V.E. (1991) in *Enzyme Mechanism from Isotope Effects* (Cook, P.F., Ed.) CRC Press, Florida.

3. Basran, J., Sutcliffe, M.J., and Scrutton, N.S. (1999) *Biochemistry 38*, 3218-3222.

4. Blanchard, C.Z., Amspacher, D., Strongin, R., and Waldrop, G. L. (1999) *Biochem. Biophys. Res. Commun. 266*, 466-471.

5. Bridger, W.A., Millen, W.A., and Boyer, P.D. (1968) *Biochemistry 7*, 3608-3616.

6. Bruice, T.C. and Benkovic, S.J. (2000) *Biochemistry 39*, 6267-6274.

7. Cornish-Bowden, A. (1995) *Fundamentals of Enzyme Kinetics*, Portland Press, London.

8. Fan, Y-X., McPhie, P., and Miles, E.W. (2000) *Biochemistry 39*, 4692-4703.

9. Galperin, M.Y. and Koonin, E.V. (1997) *Protein Sci. 6*, 2639-2643.

10. Grant, K. L. and Klinman, J.P. (1989) *Biochemistry 28*, 6597-6605.

11. Guchhait, R.B., Polakis, S.E., Hollis, D., Fenselau, C., and Lane, M.D. (1974) *J. Biol. Chem. 249*, 6646-6656.

12. Janiyani, K., Bordelon, T., Waldrop, G. L., and Cronan, J. E. Jr. (2001) *J. Biol Chem. 276*, 29864-29870.

13. Knowles, J. R. (1989) *Annu. Rev. Biochem. 58*, 195-221.

14. Koshland, D.E. (1994) *Angew. Chem. Int. Ed. Engl. 33*, 2375-2378.

15. Koshland, D.E. (1998) *Nat. Med. 4*, 1112-1114.

16. Kresge, A.J. (1977) in *Isotope Effects on Enzyme-Catalyzed Reactions* (Cleland, W.W., O'Leary, M.H., and Northrop, D.B., Eds.) University Park Press, Maryland.

17. Lane, M.D., Moss, J., and Polakis, S.E. (1974) *Curr. Top. Cell. Regul. 8*, 139-195.

18. Levert, K.L., Lloyd, R. B., and Waldrop, G.L., (2000) *Biochemistry 39*, 4122-4128.

19. Li, S-J., and Cronan, J.E. Jr. (1992) *J. Biol. Chem. 267*, 16841-16847.

20. Lorimer, F.W., Lee, E.H., Mural, R.J., Soper, T.S., and Hartmann, F.C. (1987) *J. Biol. Chem. 262*, 15327-15329.

21. Massey, V. B., Curti, B., and Ganther, H. (1965) *J. Biol. Chem. 241*, 2347-2357.

22. Melander, L., and Saunders, W.H. Jr. (1987) *Reaction Rates of Isotopic Molecules*, Robert E. Krieger Publishing, Florida.

23. Moore, W.J. (1983) *Basic Physical Chemistry*, Prentice Hall, New Jersey.

24. Shrake, A., Fisher, M.T., McFarland, P.J., and Ginsburg, A. (1989) *Biochemistry 28*, 6281-6294.

25. Sloane, V., Blanchard, C.Z., Guillot, F., and Waldrop, G.L. (2001) *J. Biol. Chem. 276*, 24991-24996.

26. Suhnel, J., and Schowen, R.L. (1991) in *Enzyme Mechanism from Isotope Effects* (Cook, P.F., Ed.) CRC Press, Florida.

27. Thoden, J. B., Blanchard, C.Z., Holden, H.M., and Waldrop, G.L. (2000) *J. Biol. Chem. 275*, 16183-16190.

28. Tipton, P.A., and Cleland, W.W. (1988) *Biochemistry 27*, 4325-4331.

29. Wakil, S.J., Stoops, J.K, and Joshi, V.C. (1983) *Annu. Rev. Biochem. 52*, 537-579.

30. Waldrop, G.L., Rayment, I., and Holden, H.M. (1994) *Biochemistry 33*, 10249-10256.

31. Wente, S.R., and Schachman, H.K. (1987) *Proc Natl. Acad. Sci. U.S.A. 84*, 31-35.

APPENDIX: RESIDUAL PLOTS

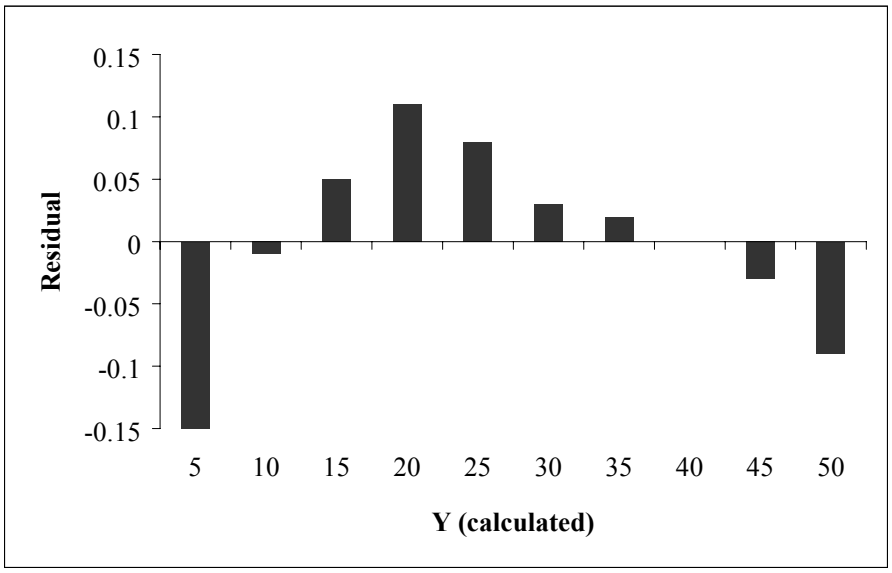

Figure 16. The residual graph showing the difference in the experimental data and calculated data for the van't Hoff plot. Temperatures are shown for reference. Note the pattern from 5-20°C and 20-50°C.

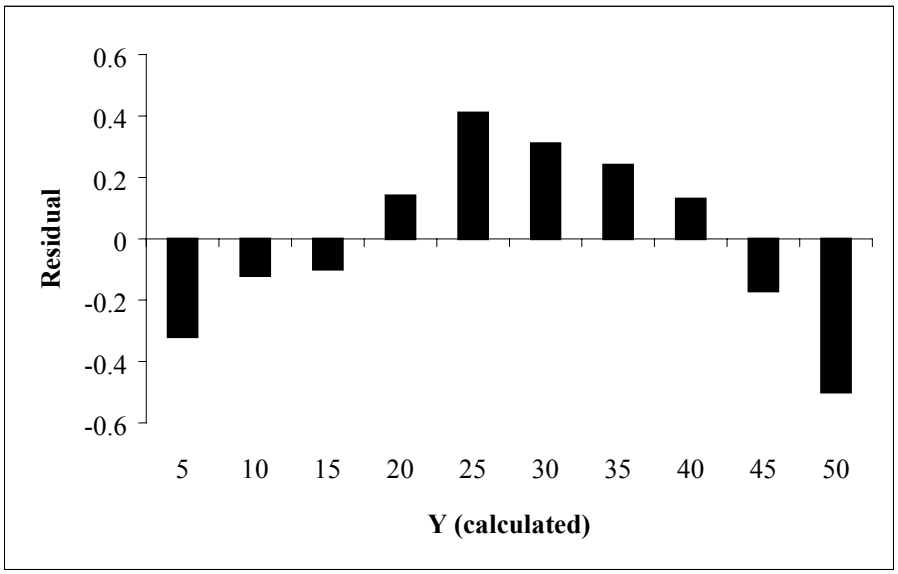

Figure 17. The residual graph showing the difference in the experimental data and calculated data for the Arrhenius plot. Temperatures are shown for reference. Note the pattern from 5-25°C and 25-50°C.

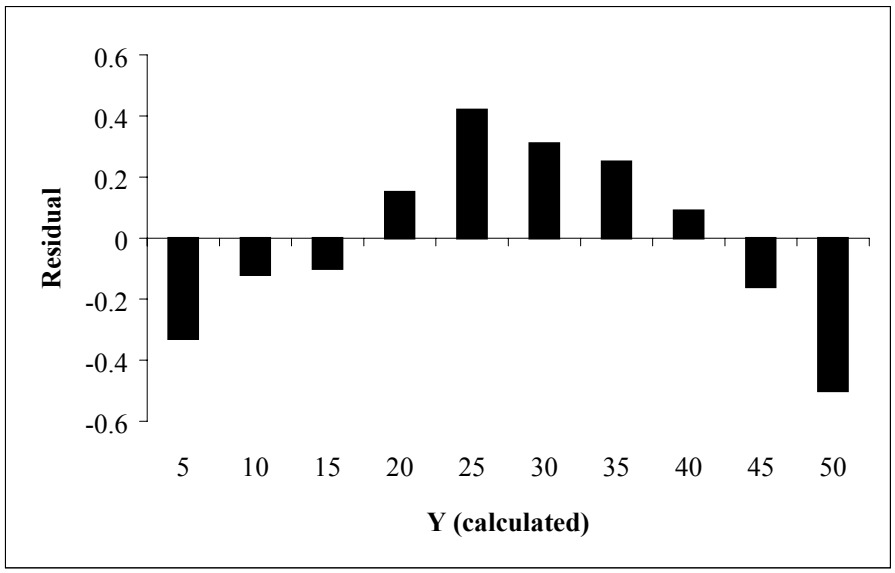

Figure 18. The residual graph showing the difference in the experimental data and calculated data for the Eyring plot. Temperatures are shown for reference. Note the pattern from 5-25°C and 25-50°C.

VITA

Brett Kenneth Lord was born on February 17, 1973, in Minneapolis, Minnesota, and raised in Mankato, Minnesota. Brett received his Bachelor of Science degree from the University of South Dakota in May 1995 and was commissioned as a Second Lieutenant in the United States Army. In August 2001, he entered the graduate program at Louisiana State University in the Department of Biological Sciences. As a graduate student, Brett worked in the laboratory of Dr. Grover L. Waldrop, where he worked on the enzyme biotin carboxylase. After graduation in May 2003, Brett will join the faculty at the United States Military Academy at West Point in the Department of Chemistry and Life Sciences as an instructor.